Monitoring of water infiltration in a reservoir sand: improving interpretation with dip steering and spectral decomposition

Paul de Beukelaar[*] and Marine Seignole of Paris-based company SoleGeo discuss a time-lapse R&D experiment using RADAR to monitor water infiltration in a reservoir sand which may have wider implications for reservoir characterization.

This article is an update of a time-lapse object detection or monitoring procedure first presented in September 2004 at the 10th European Meeting of Environmental and Engineering Geophysics, Utrecht, The Netherlands. We show here the most recent 3D and 4D interpretation results. This time lapse (4D) study consists of the geophysical interpretation of several 3D surveys at various times. Although the surveys were acquired by a RADAR method in a shallow environment, we believe the work should be of interest to seismic interpreters and more generally to geoscientists involved in reservoir characterization. The approach has proved to be an excellent illustration of powerful data interpretation techniques such as dip steering (Tingdal, 2003, Meldahl et al., 2002) and spectral analysis (Partyka et al., 1999).

The dynamic aspect of this R&D experiment consisted of water infiltration in a reservoir sand with the objective of gaining insight into a range of different reservoir sands. The first successful results were obtained with data acquired on a site in Cernay-la-Ville near Rambouillet, France. Data interpretation, using powerful analysis methods, such as dip steering attributes and spectral decomposition, led to a better understanding of the propagation of a water front depending on the petrophysical properties of a reservoir sand.

Acquisition method

Monitoring of saline water infiltration in the uppermost metre of unsaturated soil is usually done with classic electrical methods, e.g. Wenner and Schlumberger configurations (Suski et al., 2003). Direct resistivity measurements were taken before and during the infiltration of saline water. For the procedure presented here, 3D time lapse data cubes were acquired with the RADAR (RAdio Detection and Ranging), in particular, the GPR (Ground Penetrating Radar) method. This non-destructive method enables work on a small-scale and for several intervals of time. It also allows the acquisition of time-lapse data for a fraction of the budget usually needed for seismic data acquisition.

The system produces high-resolution profiles similar to those using the seismic reflection technique (if you agree). A short electromagnetic pulse in a frequency band of 10 MHZ-GHz is generated. Various waves can be observed: the air wave is the fastest (the propagation velocity of the electromagnetic waves in air is higher than in geological material). This wave type creates refracted and reflected modes due to the impedance contrasts in the soil. The direct and reflected (primary and multiples) waves are similar to those in seismic wave propagation. So, as for seismic data, it is possible to determine the impedance of a layer and the reflection coefficients. To some extent, the same methods can be used for GPR as for seismic data processing and interpretation. Some differences exist; for example, the accurate setting of the zero time position relative to the ground surface is an essential factor for the GPR data interpretation as the seismic signal is directly coupled to the ground. This position is not necessarily a fixed value. It depends on the antenna, its height above the surface, and the properties of the subsurface (Yelf, 2004). Our R&D approach demonstrates the increasing synergism in civil engineering and reservoir geophysics (de Beukelaar et al., 2004, Knight et al., 1997, Mari et al., 1999). Other interesting developments include applications of GPR data inversion to a large number of acquired GPR profiles (Saintenoy and Tarantola, 2001).

Experiment

Geometry

To create a dynamic system, an acquisition geometry and water infiltration device (Figures 1 and 2) were designed. A hole of 1 m length, with a 48° slope, was drilled into the soil. Next a PVC tube of 3 cm diameter and 1 m length was inserted. On crossline 12, the tube depth is known for each inline. In addition, since a velocity study has been done, the tube position's two-way time (twt) is also known.

Infiltration device

An injection system was inserted in the PVC tube, and during the experiment, a total of five litres of water was infiltrat-

[*] *SoleGeo, Geoscience Consultancy Services, 28 rue des Tartres, 92500 Rueil-Malmaison, France; Tel: +33 147 520 598.*

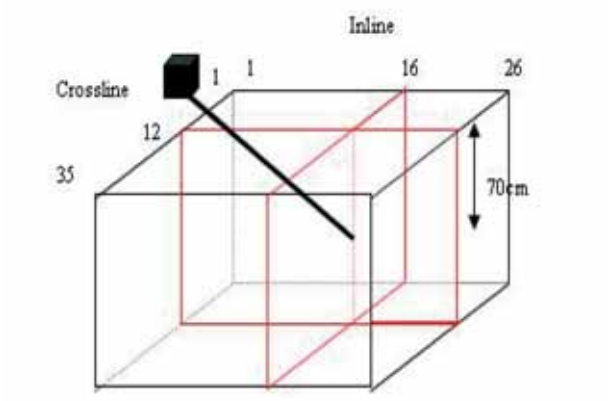

Figure 1 *3D geometry.*

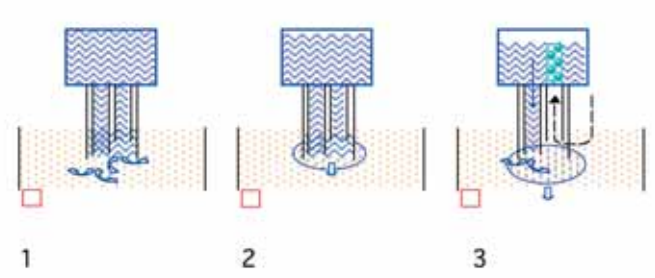

Figure 2 *Water infiltration device.*

ed in approximately 1h 30 min. A schematic view of the injection device is given in Figure 2.

It is composed of a hermetically closed water-filled tank and two soft tubes (one shorter than the other) used to inject the water. This particular device was designed so that the flow speed can be kept under control and the water prevented from creeping upwards along the walls of the pipe. Three stages can be distinguished:

- The water infiltrates into the sand. The water flow is stopped when the sand around the lower extremities of both tubes is saturated: the hydraulic pressure difference below a certain level.
- The saturation leads to a variation of pressure in the sand pore space (P increase). The bubble extends due to gravity and capillary forces until a state of balance.
- When the tube with the opening closest to this surface is not surrounded by saturated sand any more, it is replaced by air which modifies the pressure in the tank. This phenomenon leads to an increase of the pressure gradient and thus an increase of the injected flow up to the state of balance (stage 2).

Acquisition and processing

The acquisition surface has a dimension of approximately 1 m long and 75 cm wide. The acquisition was carried out along profiles (26 inlines) at a regular distance of 3 cm. The parameters of acquisition were the following:

- Antenna frequency: 800 MHz
- Sample frequency: 12671 MHz
- Number of samples: 512
- Time window: 40 ns

Three 3D surveys were acquired at different times - before infiltration at 11h40; at 12h50 (after approximately 1 litre injected); and at the end of the manipulation (after infiltration of the next 4 litres) at 13h40.

To simplify and speed up 3D acquisition to just 15 minutes per survey, a full coverage, normal incidence survey was carried out. Emitter receiver distance was only varied in a separate experiment determining wave propagation velocities. However, due to the acquisition duration, a survey is not a perfect instantaneous dataset corresponding to a certain instant of water propagation in the soil.

A basic data processing package, Seismic Unix, was used running under the Linux operating system. Scripts were created to speed up the processing of the trace-based GPR data. The scripts use a gain function, diverse filters, mute to eliminate the direct air wave, and a special data format conversion to SEG format that can be read by OpendTect (dGB).

Data analysis

Different kinds of analyses were undertaken. A traditional interpretation was carried out in a 3D cube by picking the visible hyperbolas. This method allowed a first determination of objects or possible boundaries. Dip steering is a powerful attribute analysis technique to improve object detection. A steering cube was computed in OpendTect using a sliding 3D Fourier analysis technique. The window size influences the calculation accuracy: the bigger the window, the more precise the calculation. However, this will only show a general dip or azimuth trend. The attribute 'Dip' represents the inline dip in µsec/m. The attribute 'Azimuth' represents the azimuth of the dip direction in degrees ranging from -180° to +180°. Positive azimuth is defined from the inline in the direction of increasing crossline numbers.

Spectral decomposition was a powerful tool for seismic interpretation and thickness estimation. Properties were extracted from a part of the reflectivity series through mathematical transformation - Short Window FFT and Continuous Wavelet Transform.

Figure 3 shows the results of three acquisitions: before infiltration, after approximately 1 litre injected, and at the end of the manipulation. The first five nanoseconds of the signal were muted to eliminate the direct air wave, which would mask the rest of the signal because of its strong amplitude.

In the cube acquired at 12h50, hyperbolas were picked in profile 16 (Figure 4 a); nevertheless, several interpretation choices can be made.

Following the Dip attribute computation without modifying the hyperbolas, it is getting easier to make the best inter-

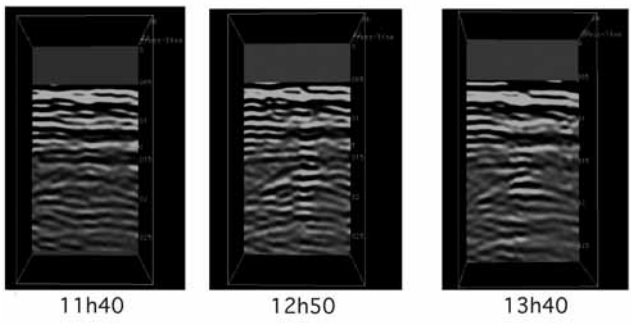

Figure 3 *Data comparison for inline 16 in chronological order of acquisition.*

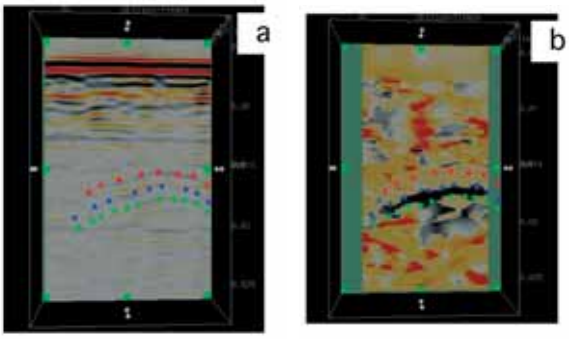

Figures 4 *Several hyperbola picking possibilities for a) processed GPR data, b) after Dip attribute computation.*

pretation choice. The blue hyperbola seems to correspond to an obvious event in the Dip attribute display (Figure 4b).

For the GPR data, the apex is situated on inline 12, cross-line 11 and 16 ns twt (8 ns one way time). For this inline, the tube's theoretical depth is equivalent to 8.3 ns. Since the geometry is known and a velocities study has been done, the twt is known. For the attribute dip, the apex is situated on inline 13, cross-line 14 and 16.5 ns twt (8.25 ns one way time). For this inline, the tube theoretical depth is equivalent to 8.7 ns. Theoretical and estimated values for the two kinds of datasets are very similar.

The base of the tube is located at inline 16, at approximately 20 ns twt. So these hyperbolas do not correspond to the end of the tube but rather to the water level in the tube. The top of the water bubble can be found on inline 12 at approximately 20 cm distance from the end of the tube.

Thanks to the dip attribute, the tube location itself can also be determined with accuracy (see Figure 6). We can identify a black area at the end of the tube: it must be the water bubble created by the 1L injected. The volume of this bubble is estimated as 0.00648 m^3 and the associated sand porosity can be computed as 16% using the following formula:

$\omega = V_{\text{water injected}} / V_{\text{bubble}}$, assuming a water saturated sand.

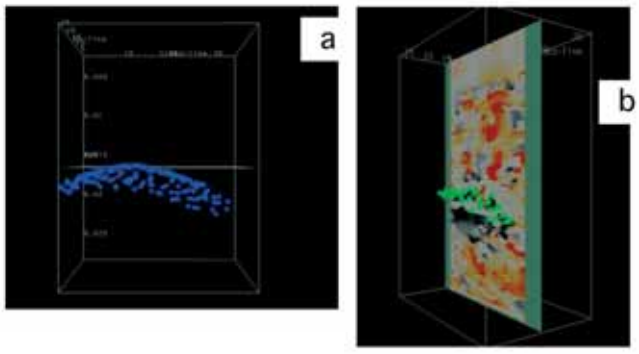

Figure 5 *Picked hyperbolas thanks to (a) GPR data (b) after Dip attribute computation. With this approach to interpretation on two data sets, hyperbolas can now be picked in all profiles.*

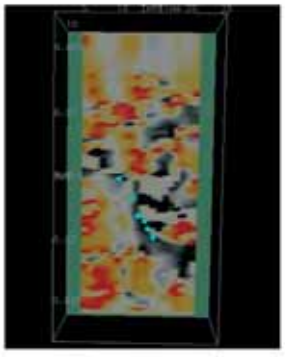

Figure 6 *Picking of tube position at crossline 12.*

Knowing that the sand porosity range is 20-30 %, water must be present before infiltration (interstitial water).

For the cube acquired at 13h40, an analysis using the Dip attribute was applied. Using the preceding method, the tube used for the infiltration can also be determined for the cube acquired at 13h40. We can identify a black area at the end of the tube, that is larger than the one in the cube of 12h40 in Figure 6.

The volume of the bubble is estimated at 0.02333 m^3. Unfortunately this bubble can't be picked in all inlines, so its volume is under-estimated. Sand porosity can be computed as 21.43 %.

Analysis using spectral decomposition

The GPR is a high frequency method with antenna of 800 MHz. The following results (Figure 8 a and b) show a time slice (20 ns) of the cube acquired at 13h40 after spectral decomposition at 6000 Hz.

Two kinds of events can be clearly identified: at the end of the tube, a particular black zone can be determined, most likely indicating a high water saturation. A 'halo' around this tube can also be picked in various time slices : it must correspond to the extreme boundary of the water bubble (Figure 8 a and b).

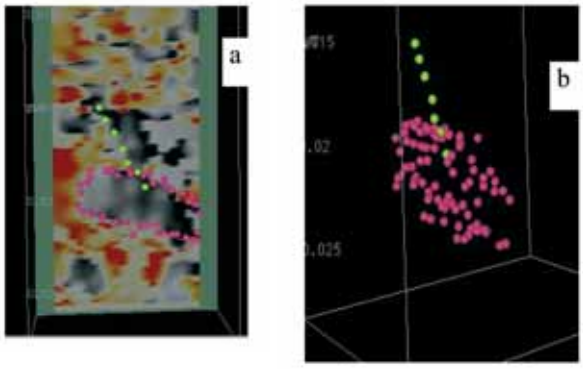

Figure 7 *Interpreted water bubble and tube a) for crossline 12, b) in 3D view after hiding the data.*

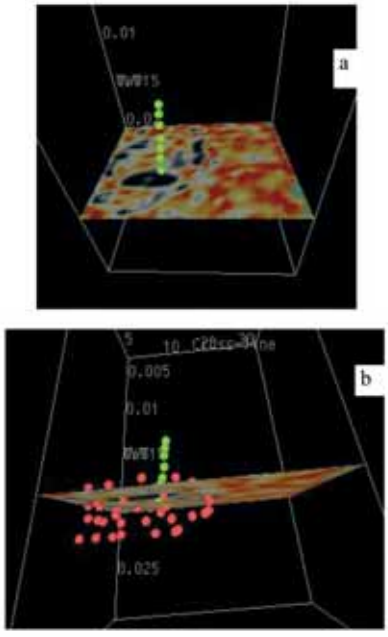

Figure 8 *Time slice 20 ns, cube acquired at 13h40 a) tube position b) tube position and Interpreted water bubble*

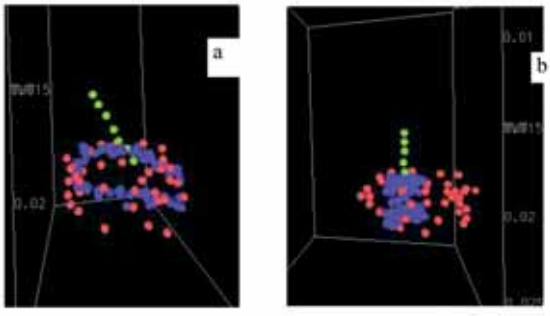

Figure 9 *Comparison between picking carried out on Spectral Decomposition data (pink) and Dip Steering data (blue)*

Picking carried out on spectral decomposition data and dip steering data are very similar. Nevertheless, the spectral decomposition method leads to a more accurate definition of the bubble. After interpreting spectral decomposition data, the volume is estimated at 0.03402 m^3 leading to an associated sand porosity of 15 %. This porosity is very similar to that estimated for the cube acquired at 12h50. Nevertheless, it is not in the 'classical' sand porosity range. This means most likely that interstitial water must be present before the infiltration experiment started.

4D interpretation

The purpose of 4D interpretation is detecting changes of petrophysical parameters. Assuming repeatability of the acquisition, observed changes should be correlated to these parameters (Oldenziel, 2003). The observed change is the bubble extension due to water infiltration. An extension rate can be determined comparing the volume after 1 L and then a further 4 L are injected. It is estimated as 9.18 10^{-5} m^3/s. Water propagation velocities can't be easily determined since the water extension is anisotropic due to gravity, capillary, and injection flow acting simultaneously, in addition to changes in petrophysical properties. However this time-lapse experiment shows excellently the spatial evolution of the non-spherical bubble shape during the water infiltration (compare figures 6 and 7a).

Conclusions and recommendations

The dip steering and the spectral decomposition seem to be powerful interpretative methods for 3D and time-lapse GPR data providing a better understanding of propagation of a water front depending on the petrophysics of a reservoir sand. Similar studies will be carried out at selected other sites during the summer of 2005, to confirm our first promising results of quantitative porosity prediction and also taking into account measurements of interstitial water in soil samples taken before infiltration. In addition, using Seismic Unix, a quantitative comparative study has still to be carried out by creating data difference cubes. Theses data sets represent the differences between the data acquired at different times (before, during and after water infiltration) and in particular also at different test sites.

It is expected that this differential cube approach will not only reveal qualitative observations like time changes of bubble shape, but also specifically depending on the type of reservoir sand. This, with accurate calibration, may also lead to further research in deriving quantitative estimates of other petrophysical parameters than porosity for different reservoir sands. The final objective of this R&D project is to gain insight into fluid propagation in different reservoir sands with their specific petrophysical parameters.

Acknowledgements

We thank in particular Albane Saintenoy (University Paris-Sud, Département Sciences de la Terre) for her contribution in GPR

acquisition and processing and also Pjotr Tucholka for his appropriate design of a steady water flow injection device. Elodie Sudriez and Gregory Meyer are thanked for writing several scripts in SU (Seismic Unix) processing. We thank Paul de Groot from dGB for his support in the use of his company's dip and azimuth plug-in for OpendTect.

References

Beukelaar de, P., Meinster, M., Meyer, G., Saintenoy, A., and Sudriez, E. [2004] 3D interpretation and cement fill monitoring using GPR over an abandoned gypsum mine. *66th EAGE Annual Conference, Paris. Extended abstracts, 1-4.*

Beukelaar de, P., Mazouz, S., Meinster M., Saintenoy A., and Tucholka P. [2004] Monitoring of water infiltration using GPR data. *10th European Meeting of Environmental and Engineering Geophysics, Utrecht. Extended abstracts, 1-4.*

Oldenziel T. [2003] *Time lapse seismic within reservoir engineering*. PhD thesis, Delft University of Technology, Department of Applied Earth Sciences.

Mari J.-L., Arens G., Chapellier D., and Gaudiani P. [1999] *Geophysics of Reservoir and Civil Engineering*. Editions Technip.

Meldahl, P., Al-Najjar, N., Oldenziel, T., and Ligtenberg, H. [2002] Semi-automated detection of 4D anomalies. *64th EAGE Annual Conference, Florence, Extended Abstracts 1-4.*

Partyka, G., Gridley, J. and Lopez, J. [1999] Interpretational applications of spectral decomposition in reservoir characterization. *The Leading Edge*, **18**, 3, 353-360.

Saintenoy A. et Tarantola A. [2001] Ground penetrating radar: analysis of point diffractors for modeling and inversion. *Geophysics*, **66**, 540-550.

Suski, B., Saintenoy, A., Tucholka, P., and Vachier, P. [2003] Monitoring of saline water infiltration in the uppermost meter of unsaturated soil using resistivity measurements. *EGS/AGU/EUG Nice*.

Tingdahl, K. [2003] Improving seismic chimney detection using directional attributes. In: Nikravesh, M., Aminzadeh, F., and Zadeh, L.A. Soft computing and intelligent data analysis in oil exploratio. *Developments in Petroleum Science*, **51**, 157-173.

Yelf, R., 2004, Where is true time zero? *Proceedings of Tenth International Conference on Ground Penetrating Radar, 21-24 June, Delft.*

SoleGeo: the company

SoleGeo was founded in 1999 as a consulting firm specializing in reservoir characterization services focused on geological knowledge, rock physics, and geophysics. Based in Paris, Solegeo recently expanded its international activities to 1) training courses in attribute analysis, inversion, quantitative evaluations, reservoir geophysics (in partnership with Fugro-Robertson and EPTS); 2) participation in risk-based projects (most recently in North Africa) based on its reservoir characterization advice work; and 3) turnkey shallow acoustic, electric tomographic, and GPR surveys (in partnership with Empec GeoSurveys).